DUAL QUARK PATTERN FOR MULTIPLICITIES AND INCLUSIVE DISTRIBUTIONS IN HADRON AND LEPTON INDUCED REACTIONS

By J. Dias de Deus

CFMC — Instituto Nacional de Investigacao Cientifica, Lisboa*

and S. Jadach**

Service de Physique Théorique, Centre d'Études Nucléaires de Saclay

(Received September 21, 1977)

Careful analysis of multiplicity, one particle inclusive spectra and resonances data leads to the idea that universality of particle production in all reactions should be abandoned and replaced by the idea of universality of quark jets. Quark jets are the building blocks in constructing production amplitudes according to the rules of duality and Topological Expansion. The model we suggest can be easily and naturally interpreted in terms of colour confinement. Multiplicities in hadron and lepton induced reactions are then related.

1. Introduction and description of the model

An inevitable consequence of the ambitious and successful Topological Expansion/Dual Unitarization scheme [1] to serve as a general framework to understand hadron physics is to be confronted with hadron multiparticle production, at first step to its most basic features represented by average multiplicity and one particle spectra.

Up to now the most attractive and simple idea has been the idea of universality [2, 3]: in all processes the bulk of the multiplicities and inclusive distributions should be the same. There are in fact qualitative features which point in that direction. The order of magnitude of the multiplicities and of their rise with energy and the shape of inclusive spectra are roughly the same in all processes. In some sense the process of hadron production seems to be universal. But on the other hand there are also differences in the actual values of multiplicities and their rate of growth with energy and in the normalized inclusive cross-

* Address: CFMO — Instituto Nacional de Investigacao Cientifica, 2 Av. Prof. Gama Pinto, Lisboa 4, Portugal.

** Permanent address: Instytut Fizyki UJ, Reymonta 4, 30-059 Kraków, Poland.

sections. We believe that these similarities and differences can be understood in the model we propose, the similarities having their origin in the universality of the colour confinement mechanism and the differences in the flavour dual structure of the production amplitudes.

The model we shall use is generally inspired by the Topological Expansion/Dual Unitarization approach [1]. However in some aspects it is extremely simplified, in other aspects it is supplemented by additional assumptions. The possible connection of TE/DU with QCD, pointed out by Veneziano [4, 5] makes it possible to interpret our model in the framework of colour confinement. The connection to the string model is then obvious. The additional assumptions mentioned above concern mainly the extension of the model to lepton induced reactions.

According to the TE/DU the most familiar multiparticle production processes, as πp, are dominated by diagram shown in Fig. 1. Through unitarity it leads to the bare Pomeron (cylinder). As demonstrated in Fig. 1 we can draw the same diagram in different

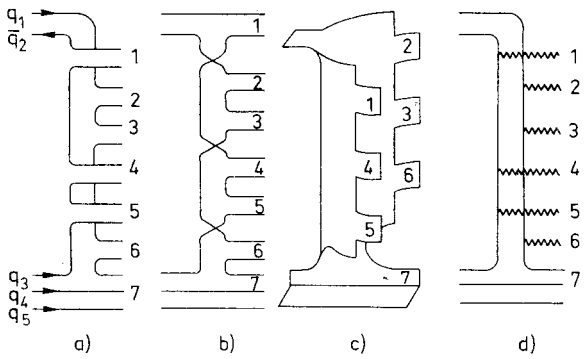

Fig. 1. Dual diagram for meson-nucleon multiple production drawn in different manners

manners (depending on a taste and emphasis). The common topological feature is that particles form two groups, (1, 4, 5) and (2, 3, 6, 7). Particles from one group, (1, 4, 5) for example, are comming from one sheet (quark line), they can resonate, we expect strong short range correlations between them. Particles from different sheets cannot resonate and are correlated weakly. We in fact assume that particles from different sheets are dynamically completely uncorrelated and we thus have production from two longitudinally allongated super-clusters which once formed decay independently. Alternatively we might think about the process as independent scattering of quarks q_2+q_3 and $q_1+q_4q_5$ leading to a double jet structure of the final state. However quarks do not interact and produce particles arbitrarily but rather following the rules of quark dual diagrams. This makes the flavour structure of production amplitudes reaction dependent.

Every jet as a whole has the definite quantum numbers of some *non-exotic* meson or baryon and can be regarded as an highly excited $q\bar{q}$ or qqq state. For low jet mass they just coincide with normal meson and baryon resonances.

We see particle production as a two step process. The first step corresponds to formation of superclusters (i. e. the split of incoming hadrons into valence quarks). The second

step is its materializing into final state pions (interaction between valence quarks and particle emission).

At this stage we can tell rather little about the first step, how the jets are formed, how is the incoming energy distributed among them. In any case we assume that the properties of the single jet, namely the multiplicity and distribution of produced particles in their own rest frame depend only on their mass and quantum numbers, and are independent of the jet origin, the same in all hadron and lepton induced reactions. We may also formulate this assumption by saying that jet formation and jet decay processes factorize in the production amplitude.

Regarding the second step, jet decay, our main assumption, mentioned before, is that each super-cluster or jet decays independently leading to separate contributions to multiplicities and particle distributions. The properties of the single jet can be learnt from experiment, because in some reactions we have only one jet and no energy distribution problem arises (e^+e^- case).

Let us now classify a few typical processes from the point of view of the dual diagram structure, see Fig. 2. The first process, Fig. 2a, is similar to the one of Fig. 1, however

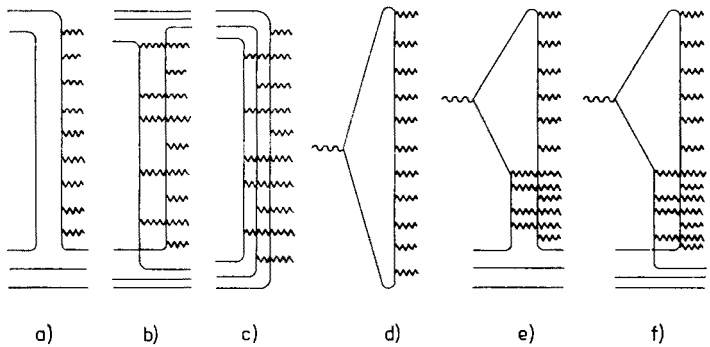

Fig. 2. Classification of few processes in terms of dual topology: a) Reggeon, b) Pomeron, c) Annihilation, d) e^+e^- annihilation, e) and f) deep inelastic production

one $q\bar{q}$ pair of valence quark instead of scattering is totally annihilated. Thus in the final state we have only one single jet with baryon quantum numbers. This diagram in the TE/DU scheme leads through the unitarity sum to Regge exchange with non-vacuum quantum numbers in the t-channel and its contribution to total cross section is vanishing as $\sigma_R/\sigma_P \sim s^{-1/2}$ as energy increases. Compared to the Pomeron contribution, Fig. 1, the Regge contribution is of second order and very good data is needed to extract it from inclusive data. An attempt is made in Section 4.

The next process, depicted in Fig. 2b, is pp collision. Only the two baryonic jet process is allowed (Pomeron). We have scattering of one valence quark of one proton with a diquark from the other (and vice versa).

In Fig. 2c we have the dominant contribution to $p\bar{p}$ annihilation. As we see all incoming quarks rearrange themselves into three $q\bar{q}$ pairs forming three jets with quantum numbers of the meson.

Figs 2d and 2e, f show e^+e^- annihilation and deep inelastic scattering. The e^+e^- annihilation is regarded as a single jet process initiated by fast $q\bar{q}$ pair. Finally in deep inelastic scattering we have two jets of different length in rapidity, see Fig. 3, one shorter is covering the rapidity from proton fragmentation region A to hole fragmentation re-

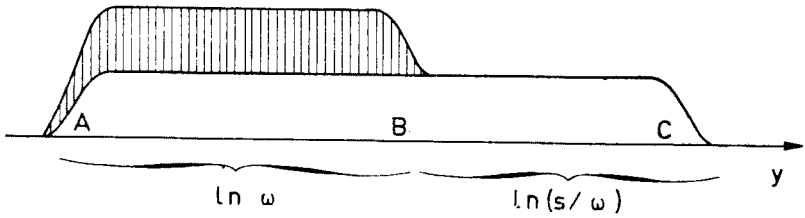

Fig. 3. Rapidity distribution in the deep inelastic production, A — proton fragmentation, B — hole fragmentation, C — struck quark fragmentation region

gion B and second, longer, covering all rapidity range from A to struck quark fragmentation region C.

As we observed the rule is simple, every s-channel sheet of the dual diagram together with valence quarks at the ends is interpreted as a single jet. The same pattern for single

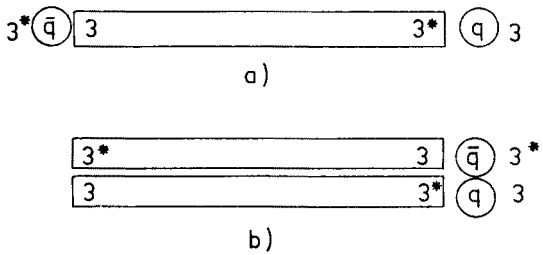

Fig. 4. Colour structure of the production mechanism: a) Reggeon, b) Pomeron

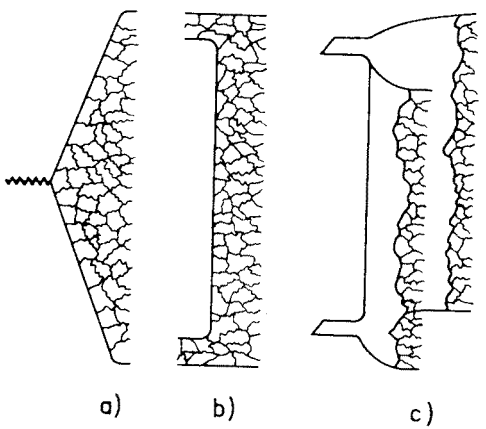

Fig. 5. Quark-gluon diagrams for a) e^+e^- annihilation, b) Reggeon, c) Pomeron

jet formation we may obtain using simple colour confinement arguments. For example in the e^+e^- annihilation case the fast growing long range potential between 3 and 3* carried by initial $q\bar{q}$ pair is screened by the tube (chain) of gluons with colour indexes arranged in such a way that colour is "locally compensated", but there is net colour charge 3 and 3* at the ends of the gluon tube. Colour of initial quarks is then balanced by the tube of gluons as it is shown schematically in Figs 4a and 5a. Tiktopulos [6] argues that in non-abelian gauge theory that sort of screening of the confining potential corresponds to the most energetically favourable situation.

To discuss hadron-hadron collision let us take meson-meson case. Neglect the sea $q\bar{q}$ pairs and assume that wee partons are at first approximation only gluons. The fast meson in principle has two simple ways of producing the chain of wee partons which are energetically favourable, i. e. screen well confining forces. First it may emit one polarized tube of gluons, but because it has unbalanced colour at the ends, one of the valence quarks must be also sent down (see Figs 4a and 5b). While passing meson target that quark annihilates one of the target valence quarks. This is Reggeon, single jet process. The second energetically favoured way of emitting wee partons is to sent down from fast meson two tubes polarized in the opposite directions, see Figs 4b and 5c, and that is obviously Pomeron, two jets process. The corresponding colour confinement picture in the case of the other processes in Fig. 2 the reader can easily construct by analogy.

The colour confinement picture allows us a better understanding of the basic assumption of our model. In particular, the universality of single jet features corresponds to strong, local in rapitity colour interaction which masks all information about the origin of the jet. On the other hand noninteraction of glue from two neighbouring jets means that we take only leading order in topological expansion [1, 4].

The rest of the paper is organized as follows. In Section 2 we discuss average multiplicities. In Section 3 we discuss one particle distributions. In Section 4 we present our conclusions.

2. *Average charged multiplicities*

The immediate consequence of the multijet structure of production amplitudes is that at asymptotic energies, $s \to \infty$, the multiplicity is, in our model, proportional to the number of jets [7] i. e.

$$\bar{n}_R = \tfrac{1}{2}\bar{n}_P = \tfrac{1}{3}\bar{n}_A \tag{1}$$

(R = Reggeon, P = Pomeron, A = Annihilation),

$$\bar{n}_R = \bar{n}_{e^+e^-} \cong \bar{n}_{ep}(\omega \to 1). \tag{2}$$

This occurs at energies high enough to neglect energy and momentum conservation and internal quantum number dependence of single jet multiplicities. At presently accessible energies care must be taken of those effects, and those low energy effects are for instance responsible for some accidental similarity of all multiplicities.

We try now to construct the charge multiplicities for the processes described in the previous section. The starting point is the single jet multiplicity which is the building block needed to construct multijet multiplicities.

The single jet multiplicity in the mesonic case is simply obtained from the e^+e^- annihilation data covering the $\sqrt{s} = 2-7.4$ GeV region [8]. The ψ point also corresponds, via Zweig-violating mixing mechanism [1], to single jet decay and is treated in the same footing. The same applies, because of duality, to the lower energy resonances ϱ, ϱ' etc. We thus extend the single jet multiplicity to the very low energy region using information on resonance decay multiplicities from Particle Data Tables. We used in this case the

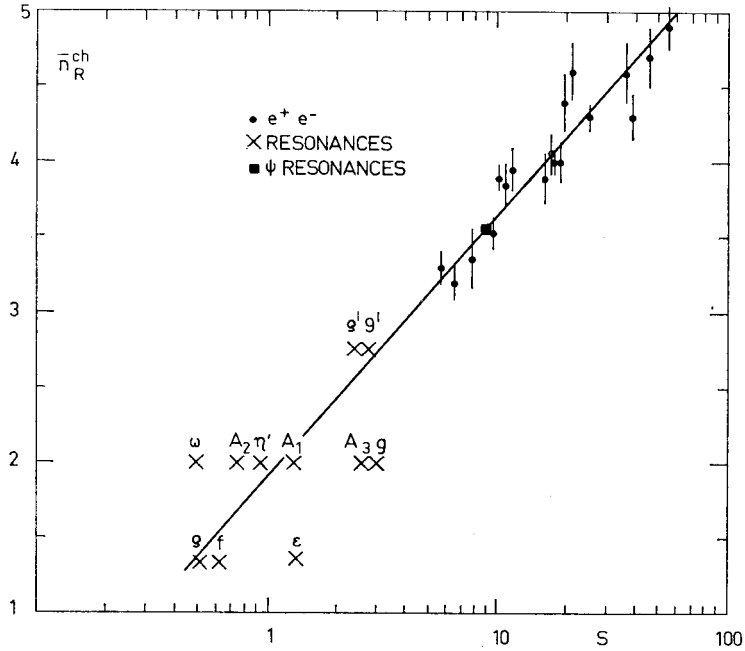

Fig. 6. Charged multiplicity for $q+\bar{q}$ jet. Plot contains e^+e^- annihilation data [8] and meson dominant decay multiplicities multiplied by factor 2/3. More strictly we treat ploted quantity as an excited $q\bar{q}$ charged multiplicity averaged over quark's isospins and that is reason why we use for resonances the factor 2/3 instead of their known charged decay multiplicity. The straight line represents "hand fit" going by definition through the ψ point

factor 2/3 to connect total multiplicities to charged ones. The result is presented in Fig. 6. The e^+e^-, the ψ and the resonance data match together in the very simple behaviour. In the logarithmic scale the straight line going through the ψ point and the middle of the other e^+e^- data points crosses the centre of the resonance data points. The obtained slope $d\bar{n}_R^{ch}/d \ln s = 0.76$ is about half of the typical hadron-hadron multiplicity slope. The same slope was also obtained from the best logarithmic fit to e^+e^- data points only, by Ferbel et al. [9]. Unfortunately we cannot include ψ' and ψ'' points in our plot. In their case apart from the planar decay, see Fig. 7a, which dominates ψ decay, we have also nonplanar

decays, of type $\psi' \to \psi$ + pions, which are visualised in Fig. 7b. Careful experimental analysis might extract pure planar multiplicity for ψ' and ψ'' but the existing data are yet not good enough.

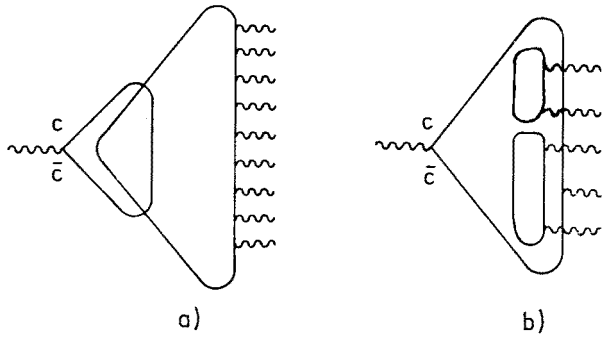

Fig. 7. Dual diagrams for a) ψ decay and $\psi' \to$ +pions decay, b) $\psi' \to \psi$+pions decay

In most applications what we need is first of all baryonic jet q+qq multiplicity. This jet should be observed in deep inelastic scattering in $\omega \to 1$ limit [10]. Data are unfortunately not at high Q^2 and s and we shall extract (or rather construct) the baryon jet multiplicity $\bar{n}_B$ using the experience from meson case. At low energies we use baryon

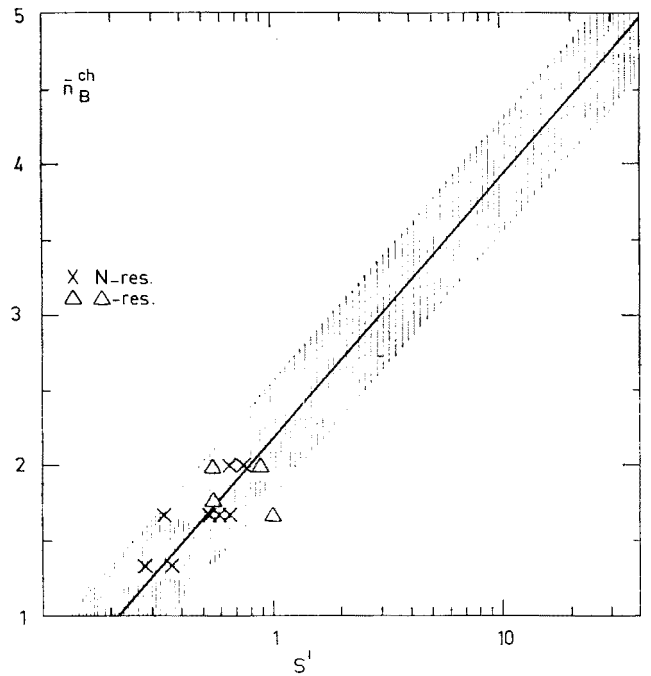

Fig. 8. Reconstruction of charged multiplicity for q+qq, baryon, type jet as a function of $s' = (\sqrt{s} - M_p)^2$. Straight line has the same slope as in Fig. 6 and by construction goes through centre of baryon resonance points. Shaded area represents uncertainty of the procedure

resonance data and at higher energies we extrapolate that data using the same slope $d\bar{n}^{ch}/d \ln s$ as in the mesonic case. However in order to get rid of large nucleon mass effect we used for logarithmic extrapolation the variable $s' = (\sqrt{s} - M_p)^2$ instead of s. The obtained extrapolation, see Fig. 8, is parametrised as $\bar{n}_B^{ch} = 0.76 \ln s' + 2.16$ while in the meson case it was $\bar{n}_R^{ch} = 0.76 \ln s + 1.90$. Within uncertainty limits the functional dependence of both, $\bar{n}_R$ and $\bar{n}_B$, is the same.

The natural assumption envolved in this procedure is that the difference between a mesonic jet and a baryonic jet occurs only at the ends of the rapidity axis, the middle of the rapidity plot is populated similarly in both cases. Later we shall also check that our $\bar{n}_B^{ch}$ is well consistent with existing deep inelastic multiplicity data in the $\omega \to 1$ limit.

Having extracted from the data $\bar{n}_R^{ch}(s)$ and $\bar{n}_B^{ch}(s)$ we can in principle apply them to construct most of the existing processes with all possible combinations of these basic jet multiplicities. The main limitation we have at this stage is that when several jets of R and/or B type are produced, we do not know a priori how the energy is shared by them. Because of that we shall try to check first if the hadron-hadron multiplicities are generally consistent with our model and our single jet multiplicities or if the model is excluded at the beginning, before we start to build anything more specific for incoming energy distribution among jets.

Let us concentrate now on pp collision for which exist the best multiplicity data [11]. In that case, because both jets are of the same, baryon type, using independence of decay assumption we may write

$$\bar{n}_{pp}^{ch}(s) = 2\bar{n}_B^{ch}(\bar{s}_B). \tag{3}$$

That equation yields also statistical approximation

$$\bar{n}_B^{ch}(\bar{s}_B) = \int \frac{1}{\sigma} \frac{d\sigma}{ds_B} \bar{n}_B^{ch}(s_B) ds_B, \tag{4}$$

where s_B is single jet mass squared. The function $\bar{s}_B(s)$ is model dependent. We shall not use any specific model and rather determine that function from Eq. (3) using at the same time $\bar{n}_{pp}$ data [11] and $\bar{n}_B$ from Fig. 8. Nevertheless the $\bar{s}_B(s)$ dependence is constrained and in the class of models consistent with our assumptions, it must possess certain features. First,

$$\bar{s} \leqslant s/4. \tag{5}$$

This is imposed by the energy conservation rule. The equality corresponds to the case when jets are at rest in the overall CM system. In the real world we may have also some energy lost in the motion of the superclusters in CM frame. Second,

$$\bar{s}_B \sim s^{\lambda}, \quad \lambda \cong 1, \tag{6}$$

in the limit $s \to \infty$. That is required by the fact that we have asymtotically average multiplicities proportional to the number of jets. The case $\bar{s}_B \sim s^{1/2}$, violating (6), would correspond to universality of multiplicities i. e. each jet populates asymptotically half of available rapidity.

From the data resulting $\bar{s}_B(s)$, depicted in Fig. 9a, meets well our expectations (5) and (6), in logarithmic scale it is approximately a straight line, with unit slope, shifted down relative to the kinematical limit $\bar{s}_B = s/4$. This means that asymptotically a fixed fraction of the available CM energy is lost in motion of jets in the CM frame. We want

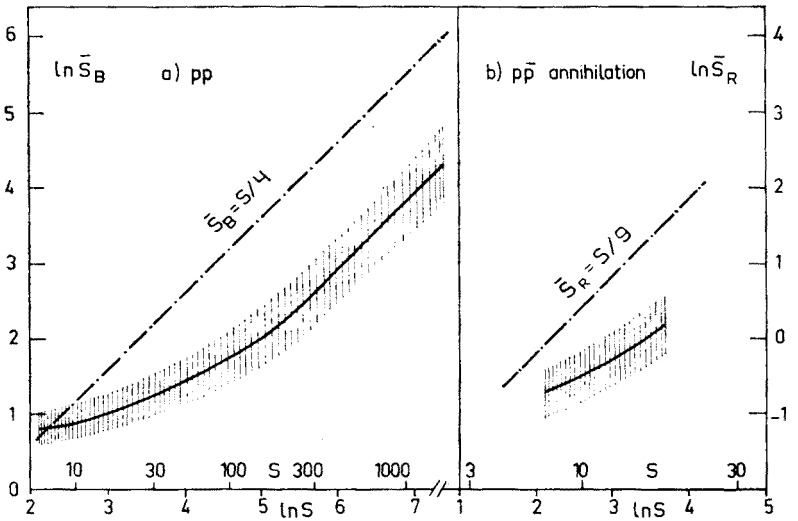

Fig. 9. a) $\bar{s}_B(s)$ dependence extracted from pp multiplicity data [11] and Fig. 7, b) $\bar{s}_R(s)$ dependence obtained using $p\bar{p}$ annihilation data [11, 12] and Fig. 6. In both cases shaded area corresponds to uncertainty depicted in Fig. 7

to stress that *our procedure relates in a logical way high energy pp multiplicity data up to a few hundred GeV/c to much lower energy e^+e^- and resonance data.*

One interesting aspect of the obtained $\bar{s}_B(s)$ dependence is its low energy limit. For example the case when $\bar{s}_B < 4$ GeV^2 roughly corresponds to two baryonic jets which are just spherical clusters coinciding with baryon resonances. That happens as we can see in Fig. 9a for quite wide range of energies, $s < 60$ GeV^2, in which we can probably well aproximate the bulk of inelastic pp production by quasi-two body production of two baryon resonances.

In the $p\bar{p}$ annihilation case we have, as we mentioned before, a three jet structure. We follow the previous prescription of determining $\bar{s}_R(s)$ through the relation

$$\bar{n}_A(s) = 3\bar{n}_R(\bar{s}_R). \tag{7}$$

Again the result is similar, see Fig. 9b, however it cannot be so convincing as in pp case because of the smaller energy range for $p\bar{p}$ annihilation data [11, 12]. Nearly at all accessible energies we have in fact rearrangement of incoming quarks into three resonances. Nonsphericity of the final state is probably mainly caused by longitudinal motion of the jets.

Unfortunately we cannot repeat that sort of analysis without more detailed model in the case when two types of jets are involved as for example one baryonic and one mesonic in the πp case.

In both cases discussed above the effective scattering energy for subscattering was much smaller than total CM energy. As an important consequence, the energy at which we expect such asymptotic phenomena like stable rapidity plateau, logarithmic growth of multiplicities might be, in hadron induced reactions, shifted to much higher energies than we expected.

The same fact may also explain the accidental similarity of all multiplicities at low energies independently of the number of the jets involved. For N jets we have very rougly

$$\bar{n}_N(s) \cong N\bar{n}(s/N^2). \tag{8}$$

Rough estimation shows that in the low s region the factor N in front and inside the argument of $\bar{n}$ tends to cancel (it is approximately true that $\bar{n} \sim s^{1/2}$ for small s). As we have already pointed out, in the available energy variable, the baryonic and mesonic jet multiplicities are quite similar. In such variable the observed multiplicity universality [2] at low s is indeed very striking. Another, more straightforward explanation of the convergence of all multiplicities at small s would be the single cluster dominance in that region. For example the typical process, independently of jet number, would be dominated by: $pp \to B^*N$, $\pi p \to \pi B^*$, $\pi p \to M^*N$, $p\bar{p} \to M^*$, $e^+e^- \to M^*$, where M^* and B^* are resonating clusters. That second possibility might have other interesting experimental consequences in the few GeV/c energy region.

The last point we shall discuss is the Q^2 dependence of the deep inelastic multiplicities. At extremely high energies we expect one particle distribution as in Fig. 3. As we observe our model explicitly breaks down Bjorken's correspondence principle [3, 13]. In our model by means of increasing Q^2 at fixed s we can vary the position of the hole region B and that will decrease the multiplicity by factor two from $Q^2 = 0$ to Q^2 very high. To discuss that in detail we should not use variable Q^2 which may vary from 0 to ∞, at fixed s, but rather the variable

$$\bar{Q}^2 = \frac{s}{\omega} = \frac{Q^2}{1 + \dfrac{Q^2}{s}}. \tag{9}$$

That variable is changing between 0 and s and its logarithm gives the length of the current plateau. At $\bar{Q}^2 = Q^2 = 0$ the deep inelastic process is dominated by Pomeron exchange and at $Q^2 \to \infty$, i. e. $\bar{Q}^2 \to s$, i. e. $\omega \to 1$ the current plateau covers all rapidity region and the process is purely planar [10]. Let us now take the deep inelastic multiplicity data [13] redrawn using variable $\bar{Q}^2$ instead of Q^2, (see Fig. 10). In the leftmost side we plot $\bar{Q}^2 = 0$ photoproduction point which match very well the deep inelastic points and in the rightmost side, at $\bar{Q}^2 = s$, we put a point taken from our $\bar{n}_B^{ch}(s)$ plot, which corresponds to purely planar multiplicity. As we see there is good agreement with electroproduction data points again. As in the hadron-induced reactions the reason why at lower energies we do not observe significant difference between one jet, $\bar{Q}^2 = 0$, and two jets, $\bar{Q}^2 = s$, multiplicities is that in spite of the fact that at $\bar{Q}^2 = 0$ we have two jets the outgoing multiplicity is not twice higher, because two jets must share among them incoming energy.

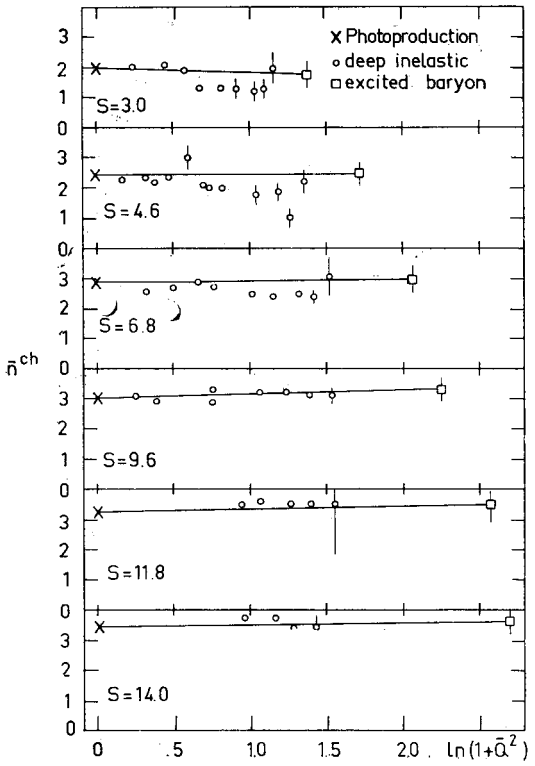

Fig. 10. Electroproduction multiplicity data [13] reploted using $\bar{Q}^2 = s/\omega$ variable. At $\bar{Q}^2 = s$ we plot $\bar{n}_B^{ch}(s)$ value from Fig. 7 with "error bar" corresponding to shaded area

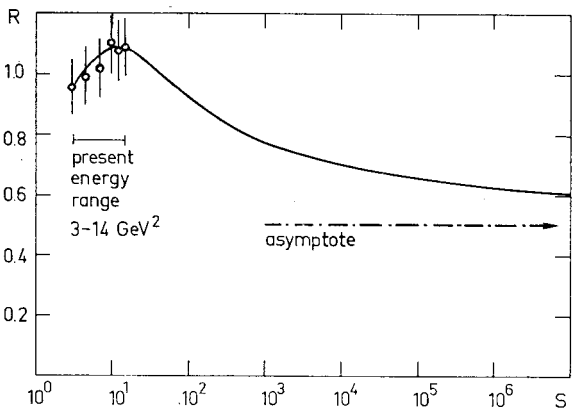

Fig. 11. The ratio $R = \bar{n}^{ch}(\bar{Q}^2 = 0)/\bar{n}^{ch}(\bar{Q}^2 = s)$ versus s. At $s < 200\ \mathrm{GeV}^2$ γp and πp data are used from Refs [11] and [13]. For $s > 200\ \mathrm{GeV}^2$ logarithmic extrapolation is used. The "data points" represent the value R taken from Fig. 10. However strictly speaking they are model dependent because for the numerator we took planar multiplicity from Fig. 8, instead of extrapolating deep inelastic data to $Q^2 \to \infty$, what should be rather uncertain with the present data

In order to see how the ratio $R = \bar{n}(\bar{Q}^2 = s)/\bar{n}(\bar{Q}^2 = 0)$ is approaching its limit $R = 1/2$ at $s \to \infty$ we ploted it taking $\bar{n}^{ch}(\bar{Q}^2 = 0) = \bar{n}^{ch}_{\gamma p} \cong \bar{n}^{ch}_{\pi p}$ and $\bar{n}^{ch}(\bar{Q}^2 = s) = \bar{n}^{ch}_{B}(s)$ at $s < 200\ \mathrm{GeV}^2$, and logarithmic extrapolation $R = (0.75 \ln s + 2.16)/(1.50 \ln s - 0.95)$ for $s > 200\ \mathrm{GeV}^2$. As we observe, see Fig. 11, the approach to the asymptotic limit is extremely slow.

Summarizing we argue that at present energies our model is as consistent with multiplicity data as the multiplicity universality model [2] or Bjorken's correspondence model [3] and we need new data at higher energies to make decisive tests.

3. One particle inclusive distributions

Having gained some confidence in handling average multiplicities in hadron and lepton induced reactions we can be more specific and look at inclusive distributions and ask more detailed questions: to what extent the single jet inclusive distribution is universal and how to construct multi-jet inclusive distributions.

When comparing hadronic data to deep inelastic or e^+e^- data, one is in fact comparing conventional hadronic physics (low p_T) to partonic physics (large p_T). And it is interesting to notice that our basic assumptions in Section 1, jets independent of their origin and independent of each other, are indeed very familiar in the parton model. Factorization of jet formation and jet decay in the production amplitude is the usual assumption of the parton model.

In the language of parton model, see for instance Ref. [14], we shall consider then the fragmentation density functions of quarks into hadrons associated with the upper (or lower) part of diagrams of Figs 1a, 2a, b, c. If $D_{h/q}(x)$ represents the probability of finding the hadron h with a longitudinal momentum fraction x of the initial quark q momentum, then the single mesonic jet inclusive density $\varrho(x)$ is related to the fragmentation function D by the equation

$$\varrho(x) = \frac{1}{\sigma} \int E \frac{d\sigma}{dp_L d^2 p_T} d^2 p_T = x D_{h/q}(x). \tag{10}$$

First we want to test the universality of the function $D_{h/q}(x)$. This test is in fact an extension to normal hadronic process of the analysis of Ref. [15] based on lepton induced reaction data.

Contrary to e^+e^- or current fragmentation in hadronic reactions one never observes the single jet isolated, but always accompanied by multijet (Pomeron) process. If $\varrho(s, x)$ is the inclusive density we have in general for an hadronic process

$$\varrho(s, x) = \sum_N \alpha_N(s) \varrho_N(x) = \alpha_1 \varrho_1(x) + \alpha_2 \varrho_2(x) + \ldots, \tag{11}$$

where $\alpha_N = \sigma_N/\sigma$ and $\sum \alpha_N = 1$. We may generalize (10) and write

$$\varrho_N(x) = x\{D_{q_1}(x) + \ldots + D_{q_N}(x)\}_N, \tag{12}$$

where $\{D(x)\}_1 = D(x)$ and $\{D(x)\}_N$ is the fragmentation function of a jet when N jets are being formed simultaneously.

We want to stress that the above split of ϱ_N into the contributions carrying flavour index q_i is an exact result of the independent decay assumption and as we shall see later in detail, the D-function is always dependent on N, otherwise energy sum rule is broken.

At the single jet contribution (Reggeon) compared to 2-jet contribution (bare Pomeron) is not dominant, $\alpha_1(s) \to 0$, $\alpha_2(s) \to 1$ as $s \to \infty$, in order to extract $\varrho_1(x)$ from (12) we have to take combinations of the inclusive experimental cross-sections and to isolate the single jet fragmentation of a meson. In practice as we want to avoid $SU(3)$ breaking and complications with diffraction we are left with pion fragmentation $\pi^- \underset{p}{\to} \pi^+$ and $\pi^+ \underset{p}{\to} \pi^-$ in $\pi^{\pm}$p collision. Knowing the quark content of the pion $\pi^+ = u\bar{d}$ and $\pi^- = d\bar{u}$, we can write, keeping only the first two terms in (11):

$$\varrho(x)|_{\pi^- \underset{p}{\to} \pi^+} = x \frac{\sigma_2}{\sigma_{\pi^- p}} \{D_{\pi^+/d}(x) + D_{\pi^+/\bar{u}}(x)\}_2 + 2x \frac{\sigma_1}{\sigma_{\pi^- p}} \{D_{\pi^+/d}(x)\}_1 \tag{13}$$

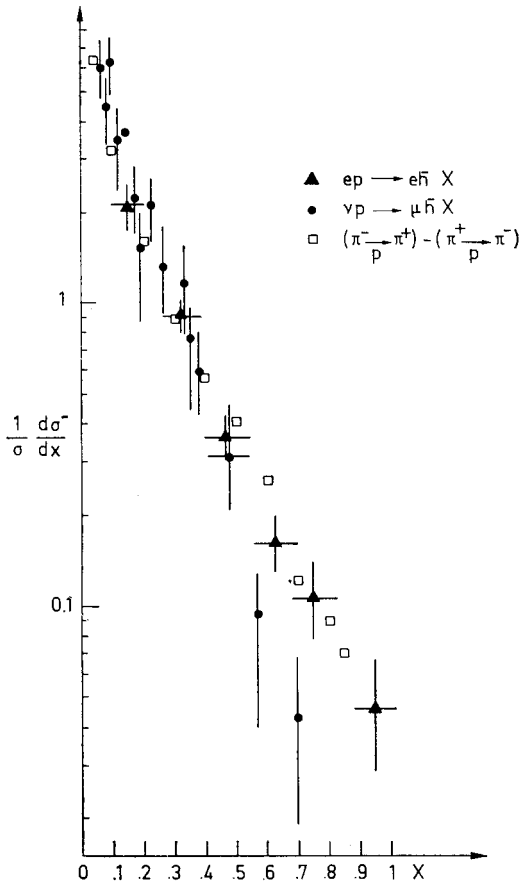

Fig. 12. $D_{\pi/u}(x)$ dependence from νp, ep, e^+e^- and πp reactions

and

$$\varrho(x)|_{\substack{\pi^+ \to \pi^- \\ p}} = x \frac{\sigma_2}{\sigma_{\pi^+ p}} \{D_{\pi^-/u}(x) + D_{\pi^-/\bar{d}}\}_2 + x \frac{\sigma_1}{\sigma_{\pi^+ p}} \{D_{\pi^-/u}(x)\}_1. \tag{14}$$

Because of isospin and charge conjugation invariance

$$D_{\pi^+/d} = D_{\pi^-/u} = D_{\pi^-/\bar{d}} = D_{\pi^+/\bar{u}}, \tag{15}$$

thus from Eqs (13), (14) and (15),

$$D_{\pi^-/u}(x) \equiv \{D_{\pi^-/u}(x)\}_1 = \frac{1}{\sigma_{\pi^- p} - \sigma_{\pi^+ p}} \left[\frac{d\sigma}{dx}\bigg|_{\substack{\pi^- \to \pi^+ \\ p}} - \frac{d\sigma}{dx}\bigg|_{\substack{\pi^+ \to \pi^- \\ p}} \right]. \tag{16}$$

A comparison between the hadronic $D_{\pi^-/u}(x)$ form the 16 GeV/c [16, 17] $\pi^{\pm}$p data and νp and ep data [15] is shown in Fig. 12. We have taken $\sigma^{\text{inel}}_{\pi^- p} = 21$ mb, $\sigma^{\text{inel}}_{\pi^+ p} = 18$ mb and we estimate the errors of our points being of 30%. The agreement between the hadronic and leptonic data is quite good, but better and different inclusive hadronic data should be used as a test in future.

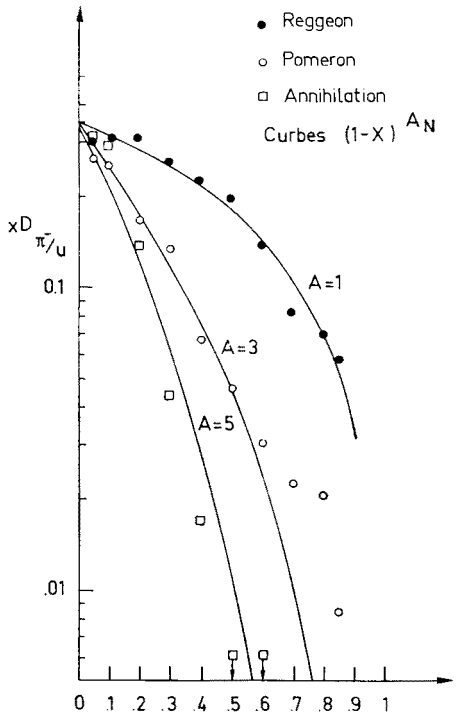

Fig. 13. $\{xD_{\pi^-/u}(x)\}_N$ function for $N = 1, 2$, and 3

Now we shall try to isolate, similarly to what we did for $\{D(x)_{\pi^-/u}\}_1$, the functions $\{D(x)_{\pi^-/u}\}_2$ and $\{D(x)_{\pi^-/u}\}_3$. For the Pomeron jet we use again the 16 GeV/c data and the relation

$$2\{xD_{\pi^-/u}(x)\}_2 = \frac{1}{\sigma_2}\left\{2x\frac{d\sigma}{dx}\bigg|_{\pi^+\to\pi^-} - x\frac{d\sigma}{dx}\bigg|_{\pi^-\to\pi^+}\right\}, \tag{17}$$

with $\sigma_2 = 2\sigma_{\pi+p} - \sigma_{\pi-p}$. For the $p\bar{p}$ annihilation jet we used 12 GeV/c $p\bar{p}$ annihilation data [19] and the relation

$$3\{xD_{\pi^-/u}(x)\}_3 = 2x\frac{1}{\sigma}\frac{d\sigma}{dx}\bigg|_{\underset{A}{p\to\pi^-}} - x\frac{1}{\sigma}\frac{d\sigma}{dx}\bigg|_{\underset{A}{p\to\pi^+}}. \tag{18}$$

In Fig. 13 we show the resulting $\{xD_{\pi^-/u}\}_1$, $\{xD_{\pi^-/u}\}_2$ and $\{xD_{\pi^-/u}\}_3$ obtained using Eqs (16), (17) and (18). One immediately sees that

$$\langle x\rangle_1 > \langle x\rangle_2 > \langle x\rangle_3, \tag{19}$$

and that all $\{xD_{\pi^-/u}\}_N$ are approximately equal only in the $x \cong 0$ region.

It is easy to see that the inequalities (19) are a consequence of energy and momentum conservation. In the very simple limit of "equipartition of momentum" the universality of single jet fragmentation and independence of jet decay advocated here, imply

$$\varrho_N(x) = N\varrho_1(x_{h/j}), \tag{20}$$

where $x_{h/j}$ is the momentum of the produced particle relative to the jet momentum, assuming that the whole jet is at rest in the C. M. frame. As $x_{h/j} = x/x_j$, x_j being the momentum fraction carried by the j-th jet (relative to $\sqrt{s}/2$) we have, in the equipartition limit, $x_j = 1/N$:

$$\varrho_N(x) = N\varrho_1(Nx) \tag{21}$$

and

$$\langle x\rangle_N \cong N\langle x\rangle_1 \tag{22}$$

and the inequalities (19) are satisfied.

The equipartition assumption is certainly too crude approximation, such strong cut-off in the longitudinal momentum does not occur and the neglecting of the motion of the whole jet is not a good approximation as we have seen in the previous section.

Generally the proper way to discuss energy and momentum conservation effects for inclusive spectra is to take energy (and momentum) sum rules. Those we write for invariant density function $\varrho(x, s) = xD(x)$ in the following simplified form

$$\int \varrho(x, s)\frac{dx}{x} = \bar{n}(s), \tag{23}$$

and

$$\int \varrho(x, s)dx = 1. \tag{24}$$

To be more specific let us write the inclusive density for N emmiting jets as

$$\varrho_N(x) = a_N(1-x)^{A_N}. \tag{25}$$

The multiplicity relation is dominated by the central $x = 0$ region and we approximately obtain,

$$\bar{n} = a_N \int (1-A_N x+ \ldots)\frac{dx}{x} = a_N(\ln s - A_N + \ldots). \tag{26}$$

In the central region energy conservation is not important, jets decay independently, and we have

$$a_N = N \times \text{const.} \tag{27}$$

The energy sum-rule on the other hand gives:

$$1 = a_N \int (1-x)^{A_N}dx = \frac{a_N}{A_N+1}. \tag{28}$$

In general one may have combination of ϱ_N's but any of them must satisfy constraints (23) and (24) separately. If the energy sum rules are to be satisfied for any value of s then we must require

$$\frac{a_N}{A_N+1} = \text{const}, \tag{29}$$

$$A_N+1 \sim N. \tag{30}$$

This simple example shows again how the energy sum rules force the shape of ϱ_N to be N dependent. This result is, of course, not specific to the particular form used for ϱ_N. In Fig. 13 we have plotted also the parametrisation of ϱ_N in the form (25) with $a_N = 0.35\,N$ and $A_N = 2N-1$ satisfying (29) and (30).

It is interesting to notice that the fact that energy and momentum conservation rule forces $\langle x_1 \rangle > \langle x_2 \rangle$ solves a well known mystery of inclusive hadronic fragmentation data. For total cross-section the ratio σ_1/σ vanishes as $s^{-1/2}$ and at intermediate energies it is of the order of few percent. At the same time for inclusive fragmentation data the ratio of the scaling violation piece over the asymptotically scaling satisfying piece which vanishes also like $s^{-1/2}$ is at the same energies surprisingly quite appreciable, even greater than one [18]. That effect is easy to understand if we notice that planar process is more peripheral and the $s^{-1/2}$ factor is easily overcomed by the $(1-x)/(1-x)^3$ factor at intermediate energies.

In this paper we limited ourselves mainly to longitudinal distributions. It would as well be interesting to study p_T distribution for multi-jet process. Using the kinematic arguments of Ref. [19] and their assumption, that every single jet has its own universal

p_T distribution relative to its own x-axis (determined by p_{Tj} and x_j of the quark which initiates j-th jet), the transverse momentum relative to normal CM x-axis is given by

$$\langle p_T^2 \rangle = a + b \left\langle \frac{1}{x_j^2} \right\rangle x^2 + \ldots, \quad 0 < x < \tfrac{1}{2}, \tag{31}$$

in which a and b are constants. In the rough "equipartition limit" $\langle 1/x_j \rangle \sim N^2$, and that gives

$$\langle p_T^2 \rangle = a + b' N^2, \tag{32}$$

which is generally consistent with the trend of the data, i. e. seagul effect is stronger in $p\bar{p}$ annihilation than in other reactions.

4. Conclusions and final remarks

From a detailed analysis of multiplicities and inclusive data we are led to develop a model for particle production easily interpreted in the framework of topological dual expansion and colour confinement. In our view high energy interactions always go via the formation of quark jets which subsequently decay by emission of mesons. The properties of the jets depend only on the intrinsic quantum numbers, mass etc. and do not depend on their origin. This feature of the jets can be related to a strong and local in rapidity colour interaction, which determines the short range structure of the final state independent of the earlier stages of the jet formation. On the other hand our quark jets decay independently i. e. there is no interaction between gluons from neighbouring jets. This property is related to suppression of the higher order terms in topological expansion as the ones originated by communication between different sheets.

Phenomenologically the model works well. In the hadronic sector $p\bar{p}$ annihilation multiplicity tends to have faster growth with ln s than any other hadronic multiplicity and that does not favour strict universality of the multiplicities. In e^+e^- annihilation multiplicity data supplemented with resonance data seems to have a slope $d\bar{n}/d\ln s$ which is half of typical hadronic, however better data at higher energies are needed to support that conjecture. The most interesting reaction is the deep inelastic scattering ep, νp, μp. Our model is clearly different from the correspondence principle of Bjorken but is not in disagreement with the data. High Q^2 and s data will provide the crucial test.

There were in the literature several attempts to relate parton ideas to conventional hadron collisions, as for example the model of Van Hove and Pokorski [20]. Similarly to them our valence quarks are weakly correlated and interact through soft gluon partons. But we strongly differ in the details of the model. For example in our case the leading outgoing nucleon in pp collision never contains all three incoming valence quarks but only two of them, the third is always from the sea. So we may have non-diffractive leading neutron as well as proton.

The picture which is emerging from recent papers [21, 4, 5] and our own works [7, 22] is somehow orthogonal to the usual multiperipheral ladder mechanism so extensively and

successfully used for Gribov-Regge type calculus in the dual unitarization scheme. The relation between those two pictures, s-channel super-cluster production and multiperipheral mechanism was discussed by Veneziano [4] in terms of the two limits of the parameter $\varrho = N_f/N_c$: $\varrho \to 0$ and $\varrho \to \infty$, (N_f and N_c are numbers of flavour and colour degrees of freedom). In fact ϱ is about one and that might explain why in the same time, $\varrho \to 0$, s-channel picture, describes well final state main feature and, $\varrho \to \infty$, multiperipheral picture, gives good results for the unitarity sum problems.

After completion of the paper we learnt from preprint by Brower et al. [23] that one of our basic assumptions, universality of single jet fragmentation distribution, as well in lepton as in hadron induced reactions was obtained as a result from two dimensional QCD model.

Outside the framework of the TE/DU scheme results in some cases similar to our own were obtained in Refs [24] and [25].

One of the authors, S. J., is grateful to Dr F. Hayot and Professor A. Morel for helpful discussion and critical remarks as well as for their hospitality at CEN-Saclay where this work was prepared.

REFERENCES

[1] H. Lee, *Phys. Rev. Lett.* **30**, 719 (1973); G. Veneziano, *Phys. Lett.* **43B**, 413 (1973); Chan Hong-Mo, J. E. Paton, *Phys. Lett.* **46B**, 228 (1973); for further references see recent reviews on dual unitarization program by Chan H. M., Rutherford Lab. Report RL-76-095.

[2] S. J. Brodsky, J. F. Gunion, *Connection Between Lepton-Induced and Hadron-Induced Multiparticle Reactions*, SLAC-PUB-1820 preprint 1976 and invited talk at Multiparticle Colloquium, Tutzing 1976; S. J. Brodsky, J. F. Gunion, *Phys. Rev. Lett.* **37**, 402 (1976).

[3] J. D. Bjorken, J. Kogut, *Phys. Rev.* **D8**, 1341 (1973).

[4] G. Veneziano, *Nucl. Phys.* **B117**, 519 (1976).

[5] G. C. Rossi, V. Veneziano, *Nucl. Phys.* **B123**, 507 (1977).

[6] G. Tiktopulos, *Phys. Lett.* **66B**, 271 (1977).

[7] J. Dias de Deus, *Nucl. Phys.* **B123**, 240 (1977).

[8] G. G. Hanson, e^+e^- *Hadron Production and Jet Structure at SPEAR*, talk at Colloquium on Multiparticle Production, Tutzing 1976.

[9] P. Stix, T. Ferbel, *Charged-Particle Multiplicities in High Energy Collisions*, Univ. of Rochester preprint COO-3065-153, 1976.

[10] E. D. Bloom, F. J. Gilman, *Phys. Rev. Lett.* **25**, 1140 (1970).

[11] E. Albini et al., *Mean Charged Multiplicities in High Energy Collisions*, Bologna preprint, November 1975.

[12] D. Gall et al., *Particle and Resonance Production in* $p\bar{p}$ *Interaction at 12 GeV/c*, DESY preprint, August 1975.

[13] P. H. Garbicius, *Phys. Rev. Lett.* **32**, 328 (1974).

[14] J. D. Bjorken, *Hadron Final States in Deep Inelastic Processes*, SLAC-PUB-1758, lectures at Summer Institute in Theoretical Physics, DESY 1975.

[15] R. D. Field, R. P. Feynman, *Phys. Rev.* **D15**, 2590 (1977).

[16] J. V. Beaupre et al., *Phys. Lett.* **37B**, 432 (1971).

[17] P. Bosetti et al., *Nucl. Phys.* **B54**, 141 (1973).

[18] R. Roberts, in *Phenomenology of Particles at High Energies*, edited by R. Cranford and R. Tenning, Academic Press, 1974.

[19] H. Satz, Y. Zarmi, *Lett. Nuovo Cimento* **15**, 421 (1976).
[20] S. Pokorski, L. Van Hove, *Acta Phys. Pol.* **B5**, 229 (1974); L. Van Hove, S. Pokorski, *Nucl. Phys.* **B86**, 243 (1975).
[21] A. H. Shehadah, E. J. Squires, *Charge Exchange and the Nature of the Pomeron*, Durham Univ. preprint, February 1977.
[22] J. Dias de Deus, S. Jadach, *Phys. Lett.* **66B**, 81 (1977).
[23] R. C. Brower, J. Ellis, M. G. Schmidt, J. H. Weis, *Phys. Lett.* **65B**, 249 (1976).
[24] K. Kinoshita, *Nuovo Cimento* **31A**, 413 (1976).
[25] N. S. Craigie, G. Preparata, *Nucl. Phys.* **B102**, 497 (1976).